

Construction of a Chromosome Map for the Phage Group II *Staphylococcus aureus* Ps55

JOHN P. BANNANTINE* AND PETER A. PATTEE

Department of Microbiology, Immunology, and Preventive Medicine,
Iowa State University, Ames, Iowa 50011

Received 13 May 1996/Accepted 13 September 1996

The genome size and a partial physical and genetic map have been defined for the phage group II *Staphylococcus aureus* Ps55. The genome size was estimated to be 2,771 kb by pulsed-field gel electrophoresis (PFGE) using the restriction enzymes *Sma*I, *Csp*I, and *Sgr*AI. The Ps55 chromosome map was constructed by transduction of auxotrophic and cryptic transposon insertions, with known genetic and physical locations in *S. aureus* NCTC 8325, into the Ps55 background. PFGE and DNA hybridization analysis were used to detect the location of the transposon in Ps55. Ps55 restriction fragments were then ordered on the basis of genetic conservation between the two strains. Cloned DNA probes containing the lactose operon (*lac*) and genes encoding staphylococcal protein A (*spa*), gamma hemolysin (*hlg*), and coagulase (*coa*) were also located on the map by PFGE and hybridization analysis. This methodology enabled a direct comparison of chromosomal organization between NCTC 8325 and Ps55 strains. The chromosome size, gene order, and some of the restriction sites are conserved between the two phage group strains.

A physical map of a chromosome consists of an ordered set of restriction fragments that places genomic sequence in the order it exists inside the cell. The resolution of chromosome structure can vary from a macrorestriction map consisting of only a few large, restriction fragments (10, 14, 17, 37) to thousands of small clones of ordered chromosomal DNA (4, 13) to a complete nucleotide sequence (11). The advantages of a physical map over a genetic map are severalfold. Physical maps are faster to construct and require considerably less labor-intensive methods. Methods in genetic mapping, such as conjugation, transformation, transduction, and mutagenesis, can be bypassed in physical map construction. Many prokaryotic physical maps have been constructed as a starting point to characterize the chromosome because methods of genetic analysis were underdeveloped (1, 2, 5, 14, 15, 17, 43, 47). Other physical maps were constructed to confirm previously established genetic maps (10, 28, 46).

With the establishment of long-range genomic mapping techniques (20, 36), there has been a recent surge in the field of prokaryotic genomic mapping. With these maps constructed, a preliminary assessment of chromosomal diversity among the prokaryotes may become possible. This assessment of chromosomal diversity has already been examined for species in the genus *Neisseria* (8), where a newly constructed *Neisseria meningitidis* map was compared with a previously constructed map of a gonococcal strain. Smith and Condemine (36) stated that "technology needs to be developed to simplify map construction by using maps that already exist for related organisms." This project outlines one such technology that was applied to *Staphylococcus aureus*.

The species is divided into five phage groups on the basis of typing patterns produced on infection with staphylococcal phages (23, 32, 33, 42, 45, 48). A detailed genetic and physical map has been established in the phage group III *S. aureus*

NCTC 8325 by using methods of classical genetics and pulsed-field gel electrophoresis (PFGE) analysis (27, 28, 31). While further characterization and refinement of the NCTC 8325 chromosome map continues, the applicability of this map to other strains of *S. aureus* belonging to other phage groups is being assessed. Some effort has been directed toward the construction of a chromosome map in a phage group I strain. Here we describe the construction of a chromosome map in the phage group II strain Ps55.

With the exception of the work done by Ralston and Baer on the modification of the host range of staphylococcal phage K₁₄ (32, 33), no DNA had been successfully transferred between *S. aureus* strains belonging to different phage groups due to restriction-modification barriers. The phage group II *S. aureus* strains in particular have always been somewhat enigmatic since they seem unable to undergo genetic exchange with other strains. This opened the possibility that they were quite divergent from other *S. aureus* strains. Martin et al. (19) attempted to map the exfoliative toxin locus in the group II strain UT0002-19 by using markers from the group III strain NCTC 8325. They could neither transform NCTC 8325 with UT0002-19 DNA nor use UT0002-19 as a recipient for DNA from NCTC 8325. In the present study, markers from NCTC 8325 were successfully transduced into the phage group II strain Ps55 by using the restriction-deficient, modification-proficient group II strain 879R4 as an intermediate host. With this approach, phage group II strains were found to be well within the overall *S. aureus* taxon, and their genetic distance was simply a consequence of strong restriction-modification barriers.

MATERIALS AND METHODS

Strains, plasmids, bacteriophages, and culture conditions. The *S. aureus* strains used are listed in Table 1. The plasmids used in this study are listed in Table 2. Phages 80 α (21) and ϕ 55 (44) were maintained by propagation on ISP8 and ISP255, respectively. Cells were grown in brain heart infusion broth (Difco Laboratories, Detroit, Mich.) or Trypticase soy broth (BBL Microbiology Systems, Cockeysville, Md.). Cells for phage propagations were grown on Trypticase soy agar (BBL Microbiology Systems) containing 5.0 mM CaCl₂. In addition, all media were enriched with thymine (20 μ g/ml) and adenine, guanine, cytosine, and uracil (each at 5 μ g/ml). Nutritional auxotrophs were scored on complete

* Corresponding author. Present address: Host-Parasite Interactions Section, Laboratory of Intracellular Parasites, Rocky Mountain Laboratories, NIAID, NIH, 903 South 4th St., Hamilton, MT 59840. Phone: (406) 363-9261. Fax: (406) 363-9204. Electronic mail address: john_bannantine@nih.gov.

TABLE 1. *S. aureus* strains used in this study

Strain	Genotype	Reference or origin
ISP8	8325-4 <i>pig-131</i>	44
ISP225	Ps55	CDC ^a
ISP479	8325-4 <i>pig-131</i> (pPQ9)	26
ISP517	8325-4 <i>pig-131 trp-164::Tn551</i>	26
ISP542	8325-4 <i>pig-131 purC193::Tn551</i>	40
ISP547	8325-4 <i>pig-131</i> Ω[Tn551]1005	ISP479 × 43°C+Em ^b
ISP580	8325-4 <i>pig-131 ilv-230::Tn551</i>	26
ISP585	8325-4 <i>pig-131 uraB232::Tn551</i>	26
ISP598	8325-4 <i>pig-131 rib-244::Tn551</i>	26
ISP691	8325-4 <i>pig-131 metC292::Tn551</i>	26
ISP794	8325-4 <i>pig-131</i>	39
ISP1024	8325-4 <i>pig-131 thrA118 trpE85</i> Ω[Tn551]1010	18
ISP1043	8325-4 <i>pig-131 tet-3490</i> Ω[Tn551]1023	18
ISP1048	8325-4 <i>pig-131</i> Ω[Tn551]1030	18
ISP1082	8325-4 <i>pig-131 nov-142 fus-149</i> Ω[Tn551]1035	18
ISP1115	8325 <i>trpE85 uraB232::Tn551 ermB327 mec-4916 nov-142 tmn-3106 rib-127</i> Ω[Tn551]1051	18
ISP1309	8325 <i>pig-131 thy-101 purA102</i> Ω[Tn551]1050	ISP1113 × ISP39 ^c
ISP1578	8325-4 <i>pig-131</i> [pTV1 (ts ^d)]	φ80αISP1577 × ISP8 ^c
ISP1768	8325-4 <i>pig-131</i> [pTV32 (ts)]	φ80αISP1767 × ISP8
ISP1779	8325-4 <i>pig-131 pan-389::Tn917</i>	ISP1578 × 43°C+Em
ISP2018	8325-4 <i>pig-131</i> [pTV32(ts)]	Cloned ISP1768 ^f
ISP2027	8325-4 <i>pig-131 lys-488::Tn917 lac</i>	ISP2018 × 43°C+Em
ISP2031	8325-4 <i>pig-131 thr-492::Tn917 lac</i>	ISP2018 × 43°C+Em
ISP2082	8325 <i>pig-131</i> Ω[Tn551]1030	φ80αISP1048 × ISP794
ISP2088	8325 <i>pig-131</i> Ω[Tn551]1023	φ80αISP1043 × ISP794
ISP2090	8325 <i>pig-131</i> Ω[Tn551]1035	φ80αISP1082 × ISP794
ISP2096	8325 <i>pig-131</i> Ω[Tn551]1050	φ80αISP1309 × ISP794
ISP2160	8325 <i>pig-131</i> Ω[Tn551]1051	ISP1115 DNA × ISP794 ^g
ISP2208	Ps55 [pTV1(ts)]	φ55/ISP2172 × ISP225
ISP2216	Ps55 <i>trp-517::Tn917</i>	ISP2208 × 43°C+Em
ISP2217	Ps55 <i>lys-518::Tn917</i>	ISP2208 × 43°C+Em
ISP2218	Ps55 <i>thr-519::Tn917</i>	ISP2208 × 43°C+Em
ISP2222	Ps55 <i>aro-521::Tn917</i>	ISP2208 × 43°C+Em
ISP2225	Ps55 <i>tyr-524::Tn917</i>	ISP2208 × 43°C+Em
ISP2343	879R4 Sps/1536 <i>fnb::Tn918</i>	Proctor ^h
ISP2363	879R4 Sps/1536 <i>fnb::Tn918 lys-488::Tn917lac</i>	φ80αISP2027 × ISP2343
ISP2370	Ps55 <i>lys-488::Tn917lac</i>	φ55/ISP2343 × ISP225
ISP2382	879R4 Sps/1536 <i>fnb::Tn918 trp-164::Tn551</i>	φ80αISP517 × ISP2343
ISP2383	879R4 Sps/1536 <i>fnb::Tn918 purC193::Tn551</i>	φ80αISP542 × ISP2343
ISP2384	879R4 Sps/1536 <i>fnb::Tn918 tyrB282::Tn551</i>	φ80αISP673 × ISP2343
ISP2386	879R4 Sps/1536 <i>fnb::Tn918 thr-492::Tn917lac</i>	φ80αISP2031 × ISP2343
ISP2387	Ps55 <i>tyrB282::Tn551</i>	φ55/ISP2384 × ISP225
ISP2389	Ps55 <i>thr-492::Tn917lac</i>	φ55/ISP2386 × ISP225
ISP2390	879R4 Sps/1536 <i>fnb::Tn918 metC292::Tn551</i>	φ80αISP691 × ISP2343
ISP2392	Ps55 <i>purC193::Tn551</i>	φ55/ISP2383 × ISP225
ISP2395	879R4 Sps/1536 <i>fnb::Tn918 ilv-230::Tn551</i>	φ80αISP580 × ISP2343
ISP2396	Ps55 <i>metC292::Tn551</i>	φ55/ISP2390 × ISP225
ISP2397	879R4 Sps/1536 <i>fnb::Tn918 rib-244::Tn551</i>	φ80αISP598 × ISP2343
ISP2399	879R4 Sps/1536 <i>fnb::Tn918 pan-389::Tn917</i>	φ80αISP1779 × ISP2343
ISP2400	Ps55 <i>ilv-230::Tn551</i>	φ55/ISP2395 × ISP225
ISP2401	Ps55 <i>rib-244::Tn551</i>	φ55/ISP2397 × ISP225
ISP2402	879R4 Sps/1536 <i>fnb::Tn918 uraB232::Tn551</i>	φ80αISP585 × ISP2343
ISP2408	Ps55 <i>pan-389::Tn917</i>	φ55/ISP2399 × ISP225
ISP2409	Ps55 <i>uraB232::Tn551</i>	φ55/ISP2402 × ISP225
ISP2410	879R4 Sps/1536 <i>fnb::Tn918</i> Ω[Tn551]1030	φ80αISP2082 × ISP2343
ISP2411	879R4 Sps/1536 <i>fnb::Tn918</i> Ω[Tn551]1035	φ80αISP2090 × ISP2343
ISP2412	Ps55 Ω[Tn551]1030	φ55/ISP2410 × ISP225
ISP2413	Ps55 Ω[Tn551]1035	φ55/ISP2411 × ISP225
ISP2414	879R4 Sps/1536 <i>fnb::Tn918</i> Ω[Tn551]1051	φ80αISP2160 × ISP2343
ISP2415	879R4 Sps/1536 <i>fnb::Tn918</i> Ω[Tn551]1050	φ80αISP2096 × ISP2343
ISP2416	879R4 Sps/1536 <i>fnb::Tn918</i> Ω[Tn551]1023	φ80αISP2088 × ISP2343
ISP2417	879R4 Sps/1536 <i>fnb::Tn918</i> Ω[Tn551]1005	φ80αISP547 × ISP2343
ISP2418	Ps55 Ω[Tn551]1051	φ55/ISP2414 × ISP225
ISP2419	Ps55 Ω[Tn551]1050	φ55/ISP2415 × ISP225
ISP2420	Ps55 Ω[Tn551]1023	φ55/ISP2416 × ISP225
ISP2421	Ps55 Ω[Tn551]1005	φ55/ISP2417 × ISP225
ISP2448	879R4 Sps/1536 <i>fnb::Tn918</i> Ω[Tn551]1010	φ80αISP1024 × ISP2343

Continued on following page

TABLE 1—Continued

Strain	Genotype	Reference or origin
ISP2449	879R4 Sps/1536 <i>fnb::Tn918</i> Ω [Tn551]40	ϕ 80 α RN1855 \times ISP2343
ISP2450	Ps55 Ω [Tn551]1010	ϕ 55/ISP2448 \times ISP225
ISP2451	Ps55 Ω [Tn551]40	ϕ 55/ISP2449 \times ISP225
RN1855	8325 <i>pig-131</i> Ω [Tn551]40	30 ^f

^a CDC, Centers for Disease Control and Prevention, Atlanta, Ga.

^b 43°C+Em denotes growth at 43°C with selection for erythromycin resistance.

^c Chromosomal DNA from ISP1113 was transformed into ISP39.

^d ts, temperature-sensitive replicon.

^e For example, phage 80 α ISP1577 \times ISP8 means that phage 80 α propagated on ISP1577 was used to transduce ISP8.

^f ISP2018 is a clone of ISP1768.

^g DNA from ISP1115 was transformed into ISP794.

^h Received from Richard A. Proctor, Department of Medical Microbiology, University of Wisconsin, Madison.

ⁱ RN1855 was obtained from Richard P. Novick, Department of Plasmid Biology, The Public Health Research Institute of New York City, Inc., New York, N.Y.

defined synthetic agar (29). When necessary, 1.5% (wt/vol) agar was added to the medium for the preparation of slants and plates.

Transduction. Bacteriophages were propagated and transductions were performed essentially as described by Schroeder and Pattee (35).

DNA preparation and restriction digestion. One percent agarose inserts were prepared as described by Patel et al. (25). Restriction digestions of inserts were performed in 250 μ l of the appropriate restriction buffer in 1.5-ml microcentrifuge tubes. Digestions using *Sma*I (New England Biolabs, Inc., Beverly, Mass.) were accomplished by the addition of 72 U of enzyme followed by incubation at 25°C for 20 h. *Sgr*AI (Boehringer Mannheim Biochemicals, Indianapolis, Ind.) digestions were incubated with 48 U of enzyme at 37°C for 4 to 5 h. *Csp*I (Promega, Madison, Wis.) digestions were performed exactly as described by the manufacturer. The time and temperature were empirically determined to be optimal at 30°C for 8 h. All digestions were stopped with 20 μ l of 0.5 M EDTA and immediately loaded onto agarose gels.

Molecular size markers. The size standard used was exclusively bacteriophage lambda concatemeric DNA (monomer = 48.5 kb). Lambda DNA was ligated into concatemers as specified by J. Iandolo (Kansas State University), with some modifications. To a 1.5-ml microcentrifuge tube were added 45 μ g of lambda *cI857ind1Sam7* DNA (New England Biolabs), 15 μ l of distilled water, 12 μ l of 10 \times ligation buffer (50 mM Tris hydrochloride [pH 7.8], 10 mM magnesium chloride, 1 mM dithiothreitol, 1 mM ATP, 50 μ g of bovine serum albumin per ml), and 6 μ l of 100 mM ATP. This mixture was incubated in a 50°C water bath for 15 min, held at 35°C for 5 min, and finally held for 5 min at room temperature. Six Weiss units of T4 DNA ligase (Promega) was added to the mixture, which was then incubated at room temperature. After 1 h, 20 μ l of 0.5 M EDTA was added to stop any further ligation. The mixture was stable on storage at 4°C for at least 3 months. The lambda DNA was loaded onto pulsed-field gels in liquid form using 3 to 4 μ l per well.

PFG. *S. aureus* chromosomal DNA fragments were separated by using a Bio-Rad CHEF-DRII (6) or TAFE apparatus (12) constructed in this laboratory. The TAFE apparatus was connected to an ISCO model 470 power supply and a Graylab model 625 timer (Cole Parmer, Chicago, Ill.), which served as the pulse switcher. The buffer cooling system consisted of a Masterflex variable speed pump (Cole Parmer) that circulated the buffer through a 15-m coil of polyethylene tubing submerged in a Lauda model RM20 bath filled with a 50% (vol/vol) water-ethylene glycol mixture. Separations were performed with a constant current of 170 mA in 1% agarose gels (SeaKem GTG agarose; FMC Bioproducts,

Rockland, Maine), using various pulse times depending on the range of resolution needed. The electrophoresis buffer was 0.25 \times TAE (1 \times TAE is 40 mM Tris-acetate and 2 mM EDTA), which was maintained at 10 to 15°C during electrophoresis.

DNA hybridization analysis. Pulsed-field gels were depurinated, denatured, and neutralized as described by Sambrook et al. (34). DNA was transferred (38) to Hybond-N nylon membranes (Amersham, Arlington Heights, Ill.) and hybridized with photoactivatable biotin (Clontech Laboratories, Palo Alto, Calif.) labeled DNA probes. Hybridization was detected by using the Blu-Gene system (Bethesda Research Laboratories, Gaithersburg, Md.).

RESULTS

Genome size estimate of Ps55. An estimate of the genome size of Ps55 was obtained by PFGE separation of chromosomal restriction fragments from *Csp*I, *Sma*I, and *Sgr*AI digestions (Fig. 1). The size of the Ps55 chromosome was determined by the sum of these restriction fragments. The fragment sizes are summarized in Table 3.

The size of the wild-type *Sma*I A fragment could not reliably be determined, even when long pulse times were used, because it migrated behind the range of resolvable lambda concatemers (data not shown). This was also true for NCTC 8325 and was solved by introducing additional *Sma*I recognition sites into the *Sma*I A fragment with *Tn917lac* (28). The *lys-488::Tn917lac* and *thr-492::Tn917lac* insertions were transferred from NCTC 8325 to Ps55 and analyzed by PFGE. The method of marker transfer was achieved in the following manner. Phage 80 α lysates prepared on various transposon-induced auxotrophs in NCTC 8325 were used to infect ISP2343 (a restrictionless phage group II strain). Phage 55 lysates prepared on these transductants were in turn used to transduce

TABLE 2. Characteristics of plasmids used in this study^a

Plasmid designation	Resistance marker(s)	Characteristics	Origin or reference
pBR322 ^{aro} ⁺	Ap ^r , Tc ^r	pBR322 + <i>S. aureus</i> chromosomal fragment that complements <i>E. coli</i> <i>aroA</i> mutants	Foster ^b
pJC09		pKK233-2 + 6-kbp <i>Hind</i> III fragment carrying <i>hlg</i>	7
pDU1192/3	Ap ^r , Tc ^r	pBR322 + 3-kbp <i>Eco</i> RI- <i>Hind</i> III fragment carrying <i>hla</i>	22
pCOA5	Ap ^r	pUC18 + 5.2-kbp fragment carrying insertionally inactive <i>coa</i>	Foster
pSPA721	Cm ^r	pACYC184 + 4.3-kbp <i>Eco</i> RI fragment carrying insertionally inactive <i>spa</i>	24
pLI1128-183	Ap ^r , Tc ^r	pBR322 + 6-kbp Ps54c chromosomal DNA fragment carrying <i>geh</i>	16
pFB34	Ap ^r , Tc ^r	pBR322 carrying phospho- β -galactosidase and other <i>lac</i> -encoded proteins	3
pTV20	Ap ^r , Cm ^r	pE194-pBR322 shuttle sequences	49
p14B8		Contains portions of the 16S + 23S rRNA genes from <i>B. subtilis</i>	41

^a *aro*, gene for aromatic amino acid biosynthesis or degradation; *hlg*, gamma lysin gene; *hla*, α -hemolysin gene; *spa*, staphylococcal protein A gene; *lac*, lactose gene or operon; *geh*, glycerolester hydrolase gene.

^b Timothy J. Foster, Department of Microbiology, Moyne Institute, Trinity College, Dublin, Ireland.

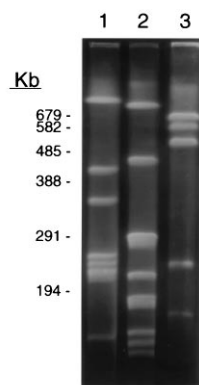


FIG. 1. Restriction fragments of Ps55 genomic DNA separated by contour-clamped homogeneous electric field electrophoresis. Lane 1, *SgrAI* restriction fragments; lane 2, *SmaI* restriction fragments; lane 3, *CspI* restriction fragments. Lambda concatemer size standards are indicated on the left.

the markers into Ps55. The validity of this technique was borne out by retention of the auxotrophic phenotype by all transposon-induced auxotrophs and rests on homologous recombination between flanking host chromosomal sequences, and not transposition, leading to the formation of recombinants. *SmaI* digestion of these Ps55 auxotrophs cleaved the A fragment into two subfragments that could be easily sized.

Mapping auxotrophic and cryptic transposon insertions. The Ps55 chromosome was physically mapped by transducing transposon insertions of known genetic and physical locations in NCTC 8325 to strain Ps55. These markers integrated into the Ps55 chromosome by homologous recombination, and their locations were determined by PFGE and hybridization analysis (Fig. 2). In instances where a silent insertion was transferred, homologous recombination could not be confirmed phenotypically. Therefore, two and sometimes three transductions of the same silent insertion were performed independently to assess the method of integration into the Ps55 chromosome (Fig. 3). The strategy to duplicate transductions of the same silent insertion was similar to that in obtaining Ps55 auxotrophs. Phage 80 α was propagated on the NCTC 8325 strain carrying the desired silent insertion and transduced

TABLE 3. *S. aureus* Ps55 fragment sizes as determined by PFGE

<i>CspI</i>		<i>SmaI</i>		<i>SgrAI</i>	
Fragment designation	Size (kb)	Fragment designation	Size (kb)	Fragment designation	Size (kb)
A	590	A	702	A	720
B	590	B	456	B	420
C	540	C	294	C	355
D	480	D	286	D	267
E	242	E	228	E	254
F	156	F	183	F	240
G	88	G	173	G	229
H	77	H	128	H	122
I	33	I	113	I	58
		J	98	J	44
		K	50	K	33
		L	43		
		M	9		
		N	6		
		O	4		
		P	3		
Total	2,796		2,776		2,742

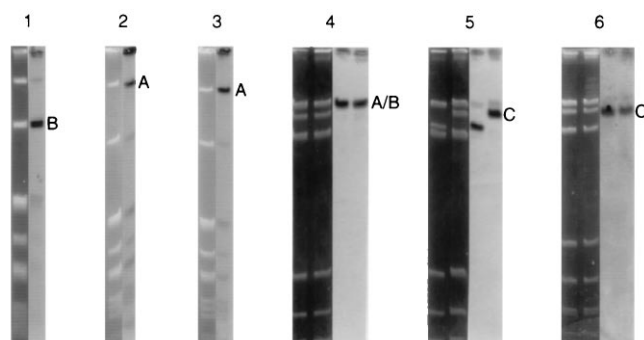


FIG. 2. PFGE and DNA hybridization of Ps55 carrying various transposon-induced auxotrophic mutations. PFGE was carried out for 15 to 16 h at 170 mA (left half of each panel) and transferred to nylon membranes (right half of each panel). Membranes were hybridized with biotinylated pTV20 DNA to detect the location of the transposon. The letters to the right of the panels indicate which restriction fragments were detected by hybridization. The hybridizations were as follows: panel 1, *SmaI*-digested ISP2392 (*purC193::Tn551*); panel 2, *SmaI*-digested ISP2222 (*aro-521::Tn917*); panel 3, *SmaI*-digested ISP2387 (*tyrB282::Tn551*); panel 4, *CspI*-digested ISP2392 (*purC193::Tn551*) and ISP2401 (*rib-244::Tn551*); panel 5, *CspI*-digested ISP2387 (*tyrB282::Tn551*) and ISP2216 (*trp-517::Tn917*); panel 6, *CspI*-digested ISP2370 (*lys-488::Tn917lac*) and ISP2389 (*thr-492::Tn917lac*).

into the group II restriction-deficient ISP2343. Two or more erythromycin-resistant (Em^r ; 10 μ g/ml) ISP2343 colonies were picked and used to propagate ϕ 55 lysates. The Em^r phenotype indicated that *Tn551* was present in the cell. The resulting lysates were used to transduce the silent insertion into Ps55. A single Em^r colony from each transduction was picked and carried through to hybridization analysis (Fig. 3). If all of the independently derived Ps55 transductants had the silent transposon element on the same restriction fragment, then it was assumed that homologous recombination and not transposition occurred. When using this strategy, we never detected transposition; homologous recombination was always found to be the method of transposon insertion into the chromosome.

The marker Ω 1030, shown in all panels of Fig. 3 (lanes 2 and 3), hybridized to the *SmaI* B fragment. Although the gel in Fig. 3A resolves the *SmaI* A and B fragments, a fragment inversion (9) between these two was identified when lanes 2 and 3 were compared in all panels. This fragment inversion occurs only between the A and B fragments, and it is reproducible at the 10-s pulse time with the TAFE apparatus. Also, the gels in Fig. 3A and C have two lanes of Ω 1030 insertions each generated independently, and in lane 3, the B fragment is shifted up approximately 70 kbp. In the wild-type Ps55 pattern, *SmaI*-B migrates between the 9th and 10th lambda multimers to a position of 456 kb, which is similar to that seen for the Ω 1030 mutant in lane 2 of Fig. 3C. The cause of this discrepancy in migration of the B fragments between otherwise identical mutants remains unknown and would be an interesting avenue for future studies. The fact remains that the B fragment was detected both times during hybridization analysis, and therefore Ω 1030 was assigned to that fragment. Much the same type of phenomenon was observed for Ω 1051 in Fig. 3C and D. With Ω 1051, the same fragment was shifted up by approximately the same number of kilobases in two of the three independently derived transductions (lanes 5 and 6). Interestingly, Ω 1051 was not found to be localized to the *SmaI* B fragment. Thus, it can be concluded that whatever caused this shift, it is reproducible and is not exclusively associated with the fragment that contains the transduced marker. The same phenomenon was observed with the *CspI* restriction pattern (data not shown). The

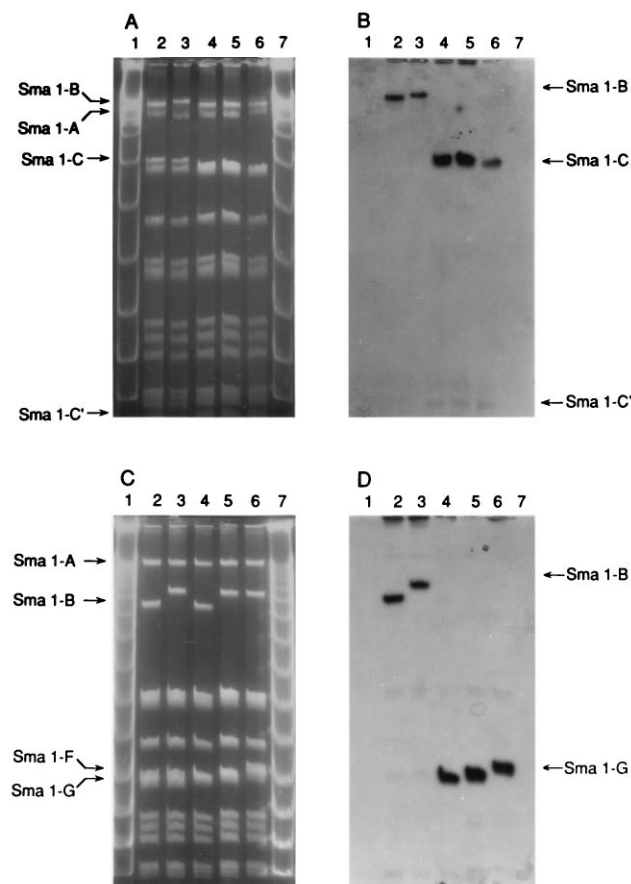


FIG. 3. PFGE and DNA hybridization of multiple, independently constructed silent *Tn551* insertions in Ps55. The gels in panel A and C were run for 13 h at 170 mA, transferred (38) to nylon membranes, and hybridized with pTV20 (B and D). *SmaI*-C' in panels A and B represents a portion of the *SmaI* C fragment that was cleaved off by an NCTC 8325 *SmaI* restriction site transduced into the Ps55 background. The A, B, and C designations in the lane assignments below indicate independently generated Ps55 transductants that carries identical markers. The pulse times are 10 and 15 s for panels A and C, respectively. Lanes in panels A and B: 1 and 7, lambda DNA multimers; 2, *SmaI*-digested ISP2412 A (Ps55 Ω [*Tn551*]1030); 3, *SmaI*-digested ISP2412 B (Ps55 Ω [*Tn551*]1030); 4, *SmaI*-digested ISP2413 A (Ps55 Ω [*Tn551*]1035); 5, *SmaI*-digested ISP2413 B (Ps55 Ω [*Tn551*]1035); 6, *SmaI*-digested ISP2413 C (Ps55 Ω [*Tn551*]1035). Lanes in panels C and D: 1 and 7, lambda DNA multimers; 2, *SmaI*-digested ISP2412 A (Ps55 Ω [*Tn551*]1030); 3, *SmaI*-digested ISP2412 B (Ps55 Ω [*Tn551*]1030); 4, *SmaI*-digested ISP2418 A (Ps55 Ω [*Tn551*]1051); 5, *SmaI*-digested ISP2418 B (Ps55 Ω [*Tn551*]1051); 6, *SmaI*-digested ISP2418 C (Ps55 Ω [*Tn551*]1051).

CspI A and B fragments comigrate as a doublet in the wild-type pattern; however, Ps55 recombinants ISP2419, ISP2450, and ISP2451 exhibited a band shift that effectively resolved this doublet. Once again the shifts were approximately 70 kbp and occurred on fragments not containing the transposon.

Fragment cleavage was observed in addition to shifting. When the marker Ω 1035 was transferred to Ps55, approximately 10 kbp was split off from one end of the *SmaI* C fragment (Fig. 3A and B). This resulted in a doublet between the C and D fragments, with the other portion of the C fragment migrating just above the *SmaI* N fragment.

The Ps55 chromosome map. The Ps55 chromosome map is shown in Fig. 4 and was assembled based on hybridization data and the assumption of gene conservation between NCTC 8325 and Ps55. In addition to locating transposon-marked loci, probes containing coagulase, lactose operon, gamma hemoly-

sin, and staphylococcal protein A coding sequences were also localized to PFGE-separated Ps55 restriction fragments by hybridization. Gene order was shown to be conserved in numerous instances based on physical data. Genetic order in Ps55 was independently confirmed by transformation analysis of selected markers (data not shown). Although the *KspI* restriction pattern generated too many restriction fragments to be clearly resolved by PFGE, the *KspI* A restriction fragment was resolved from the rest of the pattern and therefore could be confidently identified by hybridization. This *KspI* A fragment is shown on the Ps55 map, and it physically confirmed linkage between the *SmaI* C, G, and E fragments since the genes that reside on these three fragments all hybridized with *KspI*-A as well. While *SmaI*-C, -G, and -E were all found to be linked, the order of the three fragments relative to each other was uncertain. The order read clockwise was *SmaI*-E, -G, and -C if gene order is conserved between the two strains. When the *CspI* map was generated, it confirmed that E and G were adjacent because the genes that reside on *SmaI*-E and -G hybridized to the *CspI* D fragment. Physical linkages of restriction fragments were confirmed in numerous other instances as well. No data that would conflict with gene order between the two strains for any part of the map were generated. The NCTC 8325 map is also shown in Fig. 4 to facilitate comparison between the two strains.

The localization of the rRNA operons in Ps55 was performed by hybridization with a cloned probe containing the rRNA operon from *Bacillus subtilis*. Because a few *SmaI* sites were located within rRNA sequences based on junction/linking clone data (not shown), five fragments, *SmaI*-C, -F, -I, -L, and -P, were detected. Based on these data, there is an rRNA operon at the F-I junction on the Ps55 map. The locations of the *SmaI* L and P fragments could not be determined, but the rRNA hybridization data imply that they are between *SmaI* B and C and that they are linked.

The dark areas on the group II map represent regions of uncertainty. All fragments could be resolved by PFGE, but not all could be placed on the map by hybridization with a known marker from NCTC 8325. For example, none of the 8325 markers that were analyzed by hybridization in Ps55 identified the *SmaI* D, H, K, or L fragment. All of the *CspI* fragments were associated with a marker and therefore could be ordered on the Ps55 map. The *SgrAI* map is missing the E, I, and K fragments.

DISCUSSION

The goals of this project were to (i) construct a chromosome map in a representative *S. aureus* phage group II strain, (ii) evaluate the relationship of this map to that of phage group III strain NCTC 8325, and (iii) generate a preliminary assessment of chromosomal diversity within the species. At the inception of this project, little was known about the genetic organization of phage group II strains and nothing was known about Ps55. The successful transfer of DNA across phage group restriction-modification barriers by using a restriction-deficient group II strain as an intermediate host was a critical technological barrier to be overcome.

The estimated genome size of the Ps55 chromosome is 2,771 kb, which is well within the range of other bacterial chromosomes. NCTC 8325 has an estimated genome size of 2,750 kb (28), which is similar to that of Ps55.

In instances where silent insertions were transferred from NCTC 8325 to Ps55, the question of whether the silent insertion underwent homologous recombination with the isoallelic region in Ps55 had to be addressed. While this question was

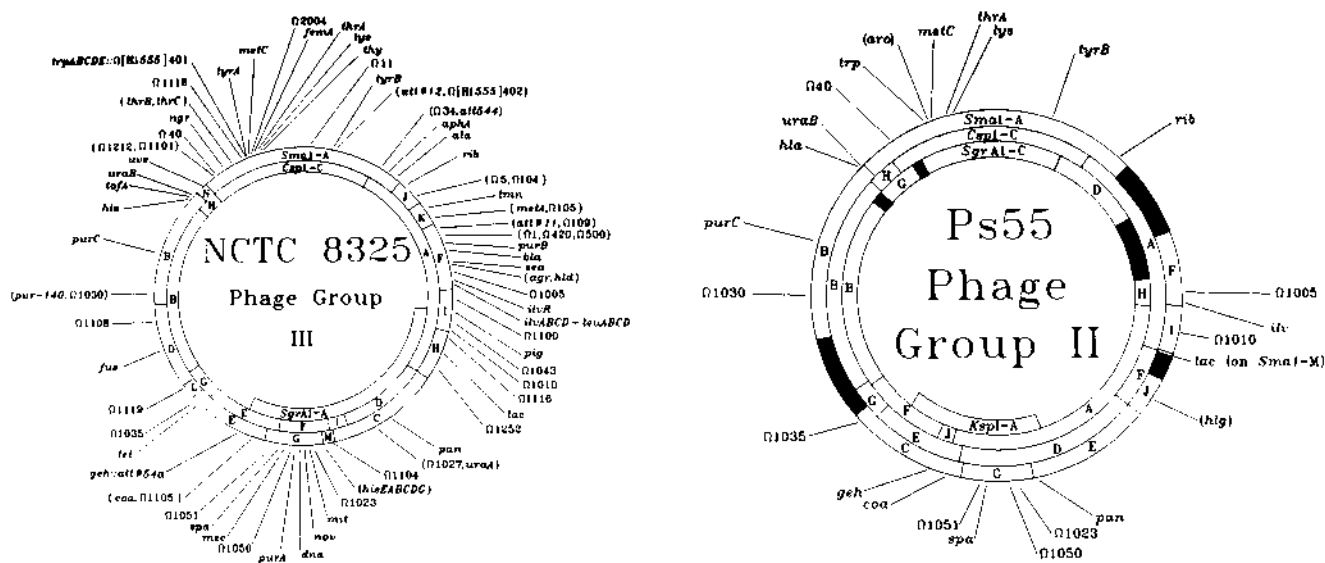


FIG. 4. The NCTC 8325 and Ps55 chromosome maps. The *Sma*I fragments comprise the outer circle, the center circle is made up of *Csp*I fragments, and the inner circle consists of *Sgr*AI fragments. The *Ksp*I A fragment is also shown for Ps55; however, no other *Ksp*I fragment could be reliably placed on the map because of the complex restriction pattern that it generates in Ps55. All fragment sizes were drawn relative to a 360° scale so that the relative sizes of the fragments would be proportional to how much of the circle they encompass. All of the markers shown for Ps55 have been physically mapped to specific restriction fragments, and the precise locations of restriction sites have not been established.

easily answered for nutritional auxotrophs by confirming the auxotrophic phenotype of the Ps55 recombinant, this technique was not applicable for silent insertions. However, PFGE analysis of two or more transductants, generated independently but carrying the same silent insert, were localized to the same restriction fragment in all instances. These data strengthen the argument that chromosomal integration occurred by homologous recombination rather than transposition.

This novel methodology of map construction involved alignment of physical and genetic data with the aid of the previously developed NCTC 8325 map. The advantage of this approach is demonstrated by the ease with which the approximate positions of restriction fragments can be determined by analyzing the DNA from many transductants on one pulsed-field gel. A limitation of this method is the absolute requirement for a series of genetic markers that are well distributed on the known chromosome map and a method of genetic exchange between the two strains. Also, this method does not allow precise alignment of restriction sites of the different enzymes used in mapping.

Throughout this project, no data that brought gene order between the two strains into question were generated. Not surprisingly, however, some restriction sites do not appear to be conserved. *Sma*I-A in Ps55, for example, extends further clockwise to encompass the riboflavin loci, whereas in NCTC 8325, the restriction site is just to the left of the loci. Also, the orientation of the NCTC 8325 *Sma*I restriction fragments E, G, and C is the opposite in Ps55 (C, G, and E read counter-clockwise), indicating that restriction site locations are similar but not exact. The *Csp*I restriction sites are remarkably conserved between the two maps. Fragment order is nearly identical with the exception of the *Csp*I F fragment location in each of the respective maps. The *spa*, Ω 1051, Ω 1050, and Ω 1023 markers have all been localized to the *Csp*I F fragment in NCTC 8325; however, those same markers are found on *Csp*I-D in Ps55. The *Csp*I F fragment is believed to be on the clockwise side of *Csp*I-A in Ps55. This result was achieved by

hybridization analysis with a junction clone which hybridized to the A and F fragments. When regions of the two maps are compared, it appears that restriction sites on the top half (from 9 o'clock to 3 o'clock) are much more conserved than those on the bottom half (from 3 o'clock to 9 o'clock) as the maps are drawn. This is probably because amino acid and other biosynthetic genes are distributed around the top half of the chromosome and these regions tend to be more conserved among species.

When the *Sma*I restriction maps of 8325 and Ps55 are compared, it is evident that at least the larger restriction fragments (A through F) appear to be in similar positions as the chromosome maps are drawn. Therefore, the Ps55 *Sma*I D fragment may be between the B and C fragments. The only other physical possibility is between the A and F fragments, hence the two black spaces in those regions.

In summary, the genomic maps of strains NCTC 8325 and Ps55 indicate that the chromosome size, gene order, and some of the restriction sites are conserved. Thus, the major difference between Ps55 and NCTC 8325 appears to be their restriction and modification systems.

ACKNOWLEDGMENTS

The assistance of Bob Evans is greatly appreciated. We thank Greg Phillips, Dan Rockey, Bob Heinzen, and Ted Hackstadt for critical review of the manuscript.

REFERENCES

1. Bancroft, I., C. P. Wolk, and E. V. Oren. 1989. Physical and genetic maps of the heterocyst-forming cyanobacterium *Anabaena* sp. strain PCC 7120. *J. Bacteriol.* **171**:5940–5948.
2. Bautsch, W. 1988. Rapid physical mapping of the *Mycoplasma mobile* genome by two-dimensional field inversion gel electrophoresis techniques. *Nucleic Acids Res.* **16**:11461–11467.
3. Breidt, F., and G. C. Stewart. 1986. Cloning and expression of the phospho- β -galactosidase gene of *Staphylococcus aureus* in *Escherichia coli*. *J. Bacteriol.* **166**:1061–1066.
4. Bukanov, N. O., and D. E. Berg. 1994. Ordered cosmid library and high-resolution physical-genetic map of *Helicobacter pylori* strain NCTC11638. *Mol. Microbiol.* **11**:509–523.

5. Canard, B., and S. T. Cole. 1989. Genome organization of the anaerobic pathogen *Clostridium perfringens*. Proc. Natl. Acad. Sci. USA **86**:6676–6680.
6. Chu, G., D. Vollrath, and R. W. Davis. 1986. Separation of large DNA molecules by contour-clamped homogeneous electric fields. Science **234**:1582–1585.
7. Cooney, J., M. Mulvey, J. P. Arbuthnot, and T. J. Foster. 1988. Molecular cloning and genetic analysis of the determinant for gamma-lysin, a two-component toxin of *Staphylococcus aureus*. J. Gen. Microbiol. **134**:2179–2188.
8. Dempsey, J. A. F., A. B. Wallace, and J. G. Cannon. 1995. The physical map of the chromosome of a serogroup A strain of *Neisseria meningitidis* shows complex rearrangements relative to the chromosomes of the two mapped strains of the closely related species *N. gonorrhoeae*. J. Bacteriol. **177**:6390–6400.
9. Ellis, T. H. N., W. G. Cleary, K. W. G. Burcham, and B. A. Bowen. 1987. Ramped field inversion gel electrophoresis: a cautionary note. Nucleic Acids Res. **15**:5489.
10. Ely, B., and C. J. Gerardot. 1988. Use of pulsed-field-gradient gel electrophoresis to construct a physical map of the *Caulobacter crescentus* genome. Gene **68**:323–333.
11. Fleischmann, R. D., M. D. Adams, O. White, R. A. Clayton, E. F. Kirkness, A. R. Kerlavage, C. J. Bult, and 33 others. 1995. Whole-genome random sequencing and assembly of *Haemophilus influenzae* Rd. Science **269**:496–512.
12. Gardiner, K., W. Laas, and D. Patterson. 1986. Fractionation of large mammalian DNA restriction fragments using vertical pulsed-field gradient gel electrophoresis. Somatic Cell Mol. Genet. **12**:185–195.
13. Kohara, Y., K. A. Kiyama, and K. Isono. 1987. The physical map of the whole *E. coli* chromosome: application of a new strategy for rapid analysis and sorting of a large genomic library. Cell **50**:495–508.
14. Krueger, C. M., K. L. Marks, and G. M. Ihler. 1995. Physical map of the *Bartonella bacilliformis* genome. J. Bacteriol. **177**:7271–7274.
15. Kuspa, A., D. Vollrath, Y. Cheng, and D. Kaiser. 1989. Physical mapping of the *Myxococcus xanthus* genome by random cloning in yeast artificial chromosomes. Proc. Natl. Acad. Sci. USA **86**:8917–8921.
16. Lee, C. Y., and J. J. Iandolo. 1986. Lysogenic conversion of staphylococcal lipase is caused by insertion of the bacteriophage L54a genome into the lipase structural gene. J. Bacteriol. **166**:385–391.
17. Lee, J. J., H. O. Smith, and R. J. Redfield. 1989. Organization of the *Haemophilus influenzae* Rd genome. J. Bacteriol. **171**:3016–3024.
18. Luchansky, J. B., and P. A. Pattee. 1984. Isolation of transposon Tn551 insertions near chromosomal markers of interest in *Staphylococcus aureus*. J. Bacteriol. **159**:894–899.
19. Martin, S. M., S. C. Shoham, M. Alsup, and M. Rogolsky. 1980. Genetic mapping in phage group 2 *Staphylococcus aureus*. Infect. Immun. **27**:532–541.
20. McClelland, M., R. Jones, Y. Patel, and M. Nelson. 1987. Restriction endonucleases for pulsed field mapping of bacterial genomes. Nucleic Acids Res. **15**:5985–6005.
21. Novick, R. P. 1963. Analysis by transduction of mutations affecting penicillinase formation in *Staphylococcus aureus*. J. Gen. Microbiol. **33**:121–136.
22. O'Reilly, M., J. C. S. de Azavedo, S. Kennedy, and T. J. Foster. 1986. Inactivation of the alpha-hemolysin of *Staphylococcus aureus* 8325-4 by site-directed mutagenesis and studies on expression of its hemolysins. Microb. Pathog. **1**:125–138.
23. Parker, M. T. 1983. The significance of phage-typing patterns in *Staphylococcus aureus*, p. 33–62. In C. S. F. Easmon and C. Adlam (ed.), Staphylococci and staphylococcal infections, vol. 1. Clinical and epidemiological aspects. Academic Press, Inc. (London) Ltd., London.
24. Patel, A. H., P. Nowlan, E. D. Weavers, and T. J. Foster. 1987. Virulence of protein A-deficient and alpha-toxin-deficient mutants of *Staphylococcus aureus* isolated by allele replacement. Infect. Immun. **55**:3103–3110.
25. Patel, A. H., T. J. Foster, and P. A. Pattee. 1989. Physical and genetic mapping of the protein A gene in the chromosome of *Staphylococcus aureus* 8325-4. J. Gen. Microbiol. **135**:1799–1807.
26. Pattee, P. A. 1981. Distribution of Tn551 insertion sites responsible for auxotrophy on the *Staphylococcus aureus* chromosome. J. Bacteriol. **145**:479–488.
27. Pattee, P. A. 1990. *Staphylococcus aureus*, p. 2.22–2.27. In Stephen J. O'Brien (ed.), Genetic maps: locus maps of complex genomes, fifth edition. Cold Spring Harbor Laboratory, Cold Spring Harbor, N.Y.
28. Pattee, P. A. 1990. Genetic and physical mapping of the chromosome of *Staphylococcus aureus* NCTC 8325, p. 163–169. In K. Drlica and M. Riley (ed.), The bacterial chromosome. American Society for Microbiology, Washington, D.C.
29. Pattee, P. A., and D. S. Neveln. 1975. Transformation analysis of three linkage groups in *Staphylococcus aureus*. J. Bacteriol. **124**:201–211.
30. Pattee, P. A., and B. A. Glatz. 1980. Identification of a chromosomal determinant of enterotoxin A production in *Staphylococcus aureus*. Appl. Environ. Microbiol. **39**:186–193.
31. Pattee, P. A., H. Lee, and J. P. Bannantine. 1990. Genetic and physical mapping of the chromosome of *Staphylococcus aureus*, p. 41–58. In R. P. Novick (ed.), Molecular biology of the staphylococci. VCH Publishers, New York, N.Y.
32. Ralston, D. J., and B. S. Baer. 1964. A new property of phage group II *Staphylococcus aureus* strains: host restriction of phage K14. J. Gen. Microbiol. **36**:1–16.
33. Ralston, D. J., and B. S. Baer. 1964. Propagation of staphylococcal typing phages on a common host, *Staphylococcus aureus* K1, and host-controlled changes in their lytic range. J. Gen. Microbiol. **36**:17–24.
34. Sambrook, J., E. F. Fritsch, and T. Maniatis. 1989. Molecular cloning: a laboratory manual. Cold Spring Harbor Laboratory, Cold Spring Harbor, N.Y.
35. Schroeder, C. J., and P. A. Pattee. 1984. Transduction analysis of transposon Tn551 insertions in the *trp-thy* region of the *Staphylococcus aureus* chromosome. J. Bacteriol. **157**:533–537.
36. Smith, C. L., and G. Condemine. 1990. New approaches for physical mapping of small genomes. J. Bacteriol. **172**:1167–1172.
37. Smith, C. L., J. G. Econome, A. Schutt, S. Kleo, and C. R. Cantor. 1987. A physical map of the *Escherichia coli* K12 genome. Science **236**:1448–1453.
38. Southern, E. M. 1975. Detection of specific sequences among DNA fragments separated by gel electrophoresis. J. Mol. Biol. **98**:503–517.
39. Stahl, M. L., and P. A. Pattee. 1983. Computer-assisted chromosome mapping by protoplast fusion in *Staphylococcus aureus*. J. Bacteriol. **154**:395–405.
40. Stahl, M. L., and P. A. Pattee. 1983. Confirmation of protoplast fusion-derived linkages in *Staphylococcus aureus* by transformation with protoplast DNA. J. Bacteriol. **154**:406–412.
41. Stewart, G. C., F. E. Wilson, and K. F. Bott. 1982. Detailed physical mapping of the rRNA genes of *Bacillus subtilis*. Gene **19**:153–162.
42. Stobberingh, E. E., and K. C. Winkler. 1977. Restriction-deficient mutants of *Staphylococcus aureus*. J. Gen. Microbiol. **99**:359–367.
43. Suwanto, A., and S. Kaplan. 1989. Physical and genetic mapping of the *Rhodobacter sphaeroides* 2.4.1 genome: genome size, fragment identification, and gene localization. J. Bacteriol. **171**:5840–5849.
44. Thompson, N. E., and P. A. Pattee. 1977. Transformation in *Staphylococcus aureus*: role of bacteriophage and incidence of competence among strains. J. Bacteriol. **129**:778–788.
45. van Boven, C. P. A., E. E. Stobberingh, J. Verhoef, and K. C. Winkler. 1974. Restriction and modification of phages in staphylococcal phage typing. Ann. N. Y. Acad. Sci. **236**:376–388.
46. Ventra, L., and A. S. Weiss. 1989. Transposon-mediated restriction mapping of the *Bacillus subtilis* chromosome. Gene **78**:29–36.
47. Wenzel, R., and R. Herrmann. 1988. Physical mapping of the *Mycoplasma pneumoniae* genome. Nucleic Acids Res. **16**:8323–8336.
48. Winkler, K. C., and C. Grooten. 1961. The relation of phage pattern and lysogenicity in the phage typing of staphylococci of phage-group II. Antonie Leeuwenhoek **27**:225–246.
49. Youngman, P. 1987. Plasmid vectors for recovering and exploiting Tn917 transpositions in *Bacillus* and other gram-positive bacteria, p. 79–103. In K. G. Hardy (ed.), Plasmids: a practical approach. IRL Press, Oxford.